Optics Communications 284 (2011) 5242–5247

Contents lists available at ScienceDirect

Optics Communications

journal homepage: www.elsevier.com/locate/optcom

# Dispersive characteristics of surface plasmon polaritons on negative refractive index gratings

M. Cuevas *, R.A. Depine

*Grupo de Electromagnetismo Aplicado, Instituto de Física de Buenos Aires, Facultad de Ciencias Exactas y Naturales, Universidad de Buenos Aires and Consejo Nacional de Investigaciones Científicas y Técnicas (CONICET), Ciudad Universitaria, Pabellón I, C1428EHA Buenos Aires, Argentina*

ARTICLE INFO

*Article history:*
Received 28 April 2011
Received in revised form 6 July 2011
Accepted 14 July 2011
Available online 29 July 2011

*Keywords:*
Surface polaritons
Plasmonics
Diffraction
Grating
Negative refraction
Metamaterials

ABSTRACT

The dispersive characteristics of surface plasmon polaritons (SPPs) supported by a periodically corrugated boundary between vacuum and a negative refractive index, isotropic material were studied theoretically by numerical solution of a dispersion equation. SPP dispersion curves were correlated with the optical response of the corrugated boundary in frequency regions where SPPs can be excited by a normally incident plane wave. Abrupt reflectivity variations, characterized by the presence of a near unity maximum and an almost zero minimum, were found in regions where the boundary without corrugation exhibits low reflectivity and rather featureless reflectivity curves.



## 1. Introduction

A surface electromagnetic wave is a confined mode of propagation along an interface separating two media. These modes are obtained as a solution to the so-called homogeneous problem, in other words, they are a solution to Maxwell's equations and the appropriate boundary conditions with no incident wave. Interest in this subject (see Ref. [1] and references therein) has long been motivated by surface plasmons polaritons (SPPs), surface waves with *p* polarization that appear when the media have dielectric permittivities $\varepsilon_1$ and $\varepsilon_2$ with opposite signs, i.e., between insulators (positive permittivity) and metals or plasmas below a critical frequency (generally complex permittivity with a negative real part). The advent of transparent artificial materials with negative refractive index [2] has aroused new interest in the study of the homogeneous problem of a surface. General conditions for the existence of SPPs at a flat interface that separates a lossless dielectric medium (constitutive parameters $\varepsilon_1>0$ and $\mu_1>0$) and a lossless, isotropic metamaterial (constitutive parameters $\varepsilon_2<0$ and $\mu_2<0$) have been presented in Ref. [3], together with the identification of new SPP regimes. These regimes correspond to different regions of the $\varepsilon-\mu$ diagram shown in Fig. 1a, where $\varepsilon=\varepsilon_2/\varepsilon_1$ and $\mu=\mu_2/\mu_1$. While regions A and C correspond to *forward* SPPs with a total-energy flux parallel to the metamaterial interface and in the same direction as wave propagation, regions B and D correspond to *backward* SPPs, for which the total energy flux parallel to the interface is opposite to the direction of wave propagation. We see that the unusual properties of NRI media are also manifested in the propagation characteristics of SPPs: flat boundaries involving transparent NRI media can support *p*- and *s*-polarized SPPs with forward and backward energy fluxes, whereas flat boundaries involving conventional media with negative permittivity can only support *p*-polarized, forward SPPs.

Since the field amplitudes decrease exponentially with the distance to the surface, the SPP propagation constant must be larger than the absolute value of the photon's wave vector in both media. This condition prevents the excitation of a surface mode with a plane wave in a plane surface. Therefore, in order to excite and detect surface modes, we must resort to special phase-coupling techniques in which the simple configuration of a single plane interface must necessarily be abandoned. The most popular phase coupling techniques [1] are based on the use of attenuated total reflection (ATR) or the use of a diffraction grating.

Due to the unusual properties of NRI media, recent investigations have begun to reexamine the SPP-photon coupling mechanism in configurations where these media are involved. The case of ATR devices has been considered in Refs. [4–7], whereas the case of transmission gratings made of NRI wires has been studied theoretically in [8]. Regarding corrugated grating couplers involving NRI media (the subject of the present paper), recent studies [9–11] have explored the connection between the propagation characteristics of SPPs supported by the coupler (as obtained from the solution to a problem *without* external excitation) and the electromagnetic

* Corresponding author.
*E-mail addresses:* rdep@df.uba.ar (M. Cuevas), rdep@df.uba.ar (R.A. Depine).

0030-4018/$ – see front matter © 2011 Elsevier B.V. All rights reserved.
doi:10.1016/j.optcom.2011.07.034

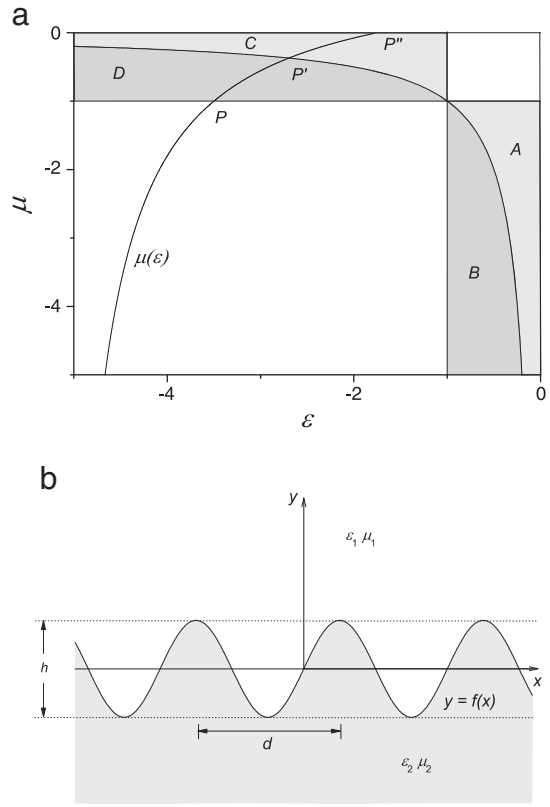


**Fig. 1.** a) SPP regimes for a flat interface between a lossless conventional material ($\varepsilon_1$ and $\mu_1$) and a lossless metamaterial with negative values of electric permittivity and magnetic permeability ($\varepsilon_2$ and $\mu_2$). The axis are $\varepsilon=\varepsilon_2/\varepsilon_1$ and $\mu=\mu_2/\mu_1$. Regions A and D correspond to *s* polarized SPPs and regions B and C correspond to *p* polarized SPPs. The curve $\mu(\varepsilon)$ gives the variation of the constitutive parameters when the frequency is varied. b) Schematic illustration of the metamaterial grating.

response of the coupler (as obtained from the solution to a problem *with* external excitation).

In the present study we focus on the dispersive – or frequency-dependent – characteristics of SPPs supported by corrugated gratings made of NRI materials, an aspect that has been overlooked in previous studies. For a conventional, metallic, grating coupler, SPP dispersion effects are essentially caused by two mechanisms. The first mechanism is associated with geometric details of the periodic boundary: the nature of conventional SPPs changes when they propagate along metal surfaces that are periodically textured on the scale of the wavelength of light [12]. In particular, when the period of the structure is half of the effective wavelength of the SPP mode, scattering may lead to the formation of SPP standing waves and the opening of an SPP stop band. The second mechanism is associated with material dispersion: metals behave ideally as an electron gas, with a frequency-dependent permittivity described by the Drude model [13]. The purpose of this paper is to investigate the combined effect that both geometric and material dispersion mechanisms have on SPPs propagating along the corrugated surface of a NRI material, an aspect which, to our knowledge, has never been considered so far.

The plan of the paper is as follows. In Section 2 we briefly review the methods used to find the SPP propagation characteristics (homogeneous problem) [14,15] and their impact on the optical response of NRI grating couplers (inhomogeneous problem) [10,16,17]. In Section 3 we show numerical results for two kinds of grating profiles: symmetric, described by a pure sinusoid, and asymmetric, described by a pure sinusoid plus its first harmonic. Assuming that the electrical permittivity and the magnetic permeability of the NRI grating follow Drude and Lorentz models respectively, we determine the SPP dispersion curves – that is, the real and the imaginary parts of the SPP propagation constant as functions of the frequency – and we correlate these results with the optical response of the surface in frequency regions where SPPs are excited by an incident plane wave. We find that, similarly to the case of metallic gratings [12,18], the periodic corrugation of the NRI medium changes the SPP dispersion curves and can lead to the formation of SPP photonic band gaps, that is, frequency ranges in which SPP propagation is forbidden. By calculating the frequency response we show that the introduction of a rather weak corrugation can dramatically change the reflectivity at normal incidence of the NRI medium. Abrupt reflectivity variations, characterized by the presence of a near unity maximum and a low value minimum, occur in a narrow frequency region where the incident wave is coupled to SPPs. When the ohmic losses of the NRI medium increase, the reflectivity maximum becomes less pronounced while the reflectivity minimum can be almost zero. Concluding remarks are provided in Section 4.

## 2. NRI grating couplers

Let us consider a SPP propagating along a periodically corrugated surface. As indicated in Fig. 1, the corrugation is represented by the function $y=f(x)$, the medium in the region $y>f(x)$ is vacuum ($\varepsilon_1=\mu_1=1$), the region $y<f(x)$ is occupied by a NRI medium characterized by the constitutive parameters $\varepsilon_2$, $\mu_2$ and the corrugation height is $h$. If $\phi(x, y)$ represents the $z$-directed component of the total magnetic field for the $p$ polarization case, or the $z$-directed component of the total electric field for the $s$ polarization case, the SPP field on each side of this surface is written as

$$\phi(x,y) = \sum_{m=-\infty}^{+\infty} R_m e^{i\left(\alpha_m x + \beta_m^{(1)} y\right)},\ y > max\{f(x)\}, \tag{1}$$

$$\phi(x,y) = \sum_{m=-\infty}^{+\infty} T_m e^{i\left(\alpha_m x - \beta_m^{(2)} y\right)},\ y < min\{f(x)\}, \tag{2}$$

where $R_m$ and $T_m$ are the complex amplitudes of the $m$th spatial harmonic,

$$\alpha_m = \alpha(h,\omega) + \frac{2\pi}{d}m, \tag{3}$$

is the $x$ component of the wave vector for the $m$-th spatial harmonic, $d$ is the corrugation period, $\beta_m^{(j)} = \sqrt{\frac{\omega^2}{c^2}\varepsilon_j\mu_j - \alpha_m^2}$, $\omega$ is the angular frequency and $\alpha(h, \omega)$ is the complex propagation constant of the SPP. For a flat surface ($h=0$), $\alpha(0, \omega)$ can be obtained analytically in terms of the relative constitutive parameters $\varepsilon$ and $\mu$ [3]. When losses are neglected, $\alpha(0, \omega)$ is real. In this case the general conditions for the existence of SPPs are indicated in the $\varepsilon-\mu$ space shown in Fig. 1a. However, even in the case of lossless media, the interaction between the SPP and the periodic corrugation can induce a non-null imaginary part in the propagation constant of the spatial harmonics and, consequently, the SPP loses energy as it propagates. In general, the interaction SPP-corrugation is stronger when Bragg's condition is satisfied,

$$\frac{d}{2\pi}\mathrm{Re}\ \alpha(h,\omega) = \frac{n}{2}, \qquad n\ \text{an integer},\ \xi(n)\neq 0, \tag{4}$$

where $\xi(n)$ is the $n$-th Fourier coefficient of the corrugation function $f(x)$. For metallic gratings [19,20,18], a forbidden frequency band gap for SPP propagation is opened under these circumstances.

In order to obtain the complex values of $\alpha(h, \omega)$ we have developed a perturbative method valid in the small roughness limit ($h/\lambda \ll 1$, where $\lambda=2\pi/\omega$ is the wavelength in vacuum) [15]. Taking into account that for $h=0$ the SPP is described by the spatial harmonic with $m=0$, the amplitude corresponding to this harmonic results O (1) in the weak corrugation limit, while the amplitudes for harmonics

with $m \neq 0$ are at least $O(h/\lambda)$. By retaining the first-order terms in the series Eqs. (1) and (2) the dispersion relation for the spatial harmonic $m=0$ is written as [15]

$$M_{00} = \beta_0^{(2)} + \sigma\beta_0^{(1)} = -\sum_{m\neq 0} \frac{M_{0m}\, M_{m0}}{M_{mm}} \left(\beta_m^{(1)} - \beta_0^{(2)}\right)\left(\beta_0^{(1)} - \beta_m^{(2)}\right) |\xi^{(1)}(m)|^2, \quad (5)$$

where $\sigma=\varepsilon$ for $p$ polarization, $\sigma=\mu$ for s polarization and the matrix

$$M_{mn} = \beta_n^{(2)} + \sigma\beta_m^{(1)} + \frac{(\alpha_m + \sigma\alpha_n)(\alpha_m - \alpha_n)}{\beta_m^{(1)} - \beta_n^{(2)}}. \quad (6)$$

To solve this dispersion Eq. (5), we used an iterative method initialized with the value $\alpha(0, \omega)$ corresponding to the flat interface. Particular care must be taken to choose the physical Riemann sheets corresponding to $\beta_m^{(j)}$, $j=1, 2$ [14].

As we are interested in correlating the propagation characteristics of SPPs with the electromagnetic response of the periodic structure, we next consider that the grating is illuminated from the vacuum side by a linearly polarized wave forming an angle $\theta$ with the $y$ axis. Outside the corrugations, $|y|>h/2$, both the reflected and the transmitted fields are rigorously represented by a series of spatial harmonics, identical in form to those given in Eqs. (1) and (2), except for the following two changes: i) the wave numbers

$$\alpha_m = \frac{\omega}{c}\sin\theta + \frac{2\pi}{d}m, \quad (7)$$

are now real numbers related to the angle of incidence, and not the complex numbers given by Eq. (3) related to the SPP propagation constant; and ii) the complex amplitudes $R_m$ and $T_m$ now correspond to the amplitudes of the reflected and transmitted orders [17], and not to the amplitudes of the $m$-th spatial harmonic of the SPP. Note that only a finite number of reflected and transmitted orders corresponds to propagating plane waves while the others have an evanescent nature.

A coupling between the incident field and a SPP propagating along the surface with complex propagation constant $\alpha(h, \omega)$ can occur when one of the evanescent orders is phase matched with the SPP. The coupling condition can be written as

$$\frac{\omega}{c}\sin\theta + \frac{2\pi}{d}m = \mathrm{Re}\ \alpha(h,\omega), \quad (8)$$

where $m$ is an integer. In terms of the dimensionless propagation constant $(d/2\pi)\mathrm{Re}\ \alpha$ and for normal incidence this condition can be rewritten as

$$m = \frac{d}{2\pi}\mathrm{Re}\ \alpha(h,\omega). \quad (9)$$

## 3. Results

To investigate the dispersion characteristics of SPPs supported by a NRI grating and the impact that these SPPs have on the grating electromagnetic response, in this section we give numerical examples obtained by using the formalisms sketched above.

Regarding SPP dispersion effects, we have considered those having a geometric as well as a material origin. To illustrate the geometric effects associated with the details of the periodic boundary, we present results corresponding to symmetric, sinusoidal corrugations (Section 3.1) and results corresponding to asymmetric corrugations represented by a pure sinusoid plus its first harmonic (Section 3.2). To illustrate the material effects associated with the dispersive nature of the electrical permittivity and the magnetic permeability of the NRI material, we assume that $\varepsilon_2(\omega)$ is represented by Drude's model

$$\varepsilon_2(\omega) = 1 - \frac{\omega_p^2}{\omega^2 + i\ \gamma\ \omega}, \quad (10)$$

and that $\mu_2(\omega)$ is represented by the following expression

$$\mu_2(\omega) = 1 - \frac{F\omega^2}{\omega^2 - \omega_0^2 + i\ \gamma\ \omega}, \quad (11)$$

where $\gamma$ is the damping constant and $\omega_p$ and $\omega_0$ are the plasma frequency and the magnetic resonance frequency respectively. In Fig. 1a we show the $\mu(\varepsilon)$ curve used in the examples for ideal NRI media, obtained for parameters $\omega_0/\omega_p=0.4$, $F=0.56$ and $\gamma=0$. For frequencies in the range $0.471<\omega/\omega_p<0.6$, the $\mu(\varepsilon)$ curve falls on regions C and D of the $\varepsilon-\mu$ space. When $\omega$ varies in the interval $0.471<\omega/\omega_p<0.52$, a point in the curve $\varepsilon(\mu)$ moves from point $P$ to point $P'$, within the region corresponding to $s$-polarized, backward SPPs. Similarly, when $\omega$ varies in the interval $0.52<\omega/\omega_p<0.6$, a point in the curve $\varepsilon(\mu)$ moves from point $P'$ to point $P''$, within the region corresponding to $p$-polarized, forward SPPs. Since the dispersion equation gives two complex solutions differing in sign (for propagation along $\pm x$), we have chosen to plot the dispersion curve for the dimensionless propagation constant $(d/2\pi)\alpha(h,\omega)$ with a positive real part.

Regarding the impact that these SPPs may have on the electromagnetic response of the NRI grating, we correlate the SPP dispersion curves with the reflectivity curves obtained when the NRI grating is illuminated by a normally incident plane wave. In all the examples we have chosen the period of the corrugation so that the grating reflects just the specular order.

### 3.1. Symmetric corrugations

Let us consider a sinusoidal corrugation represented by $f(x) = \frac{h_0}{2}\sin(\frac{2\pi}{d}x)$. In this case the corrugation height is $h=h_0$. In Fig. 2a ($\mathrm{Re}\ \alpha(h, \omega)$) and b ($\mathrm{Im}\ \alpha(h, \omega)$) we show the SPP dispersion curves with different values for the damping constant $\gamma$ in Eqs. (10) and (11)) with $h_0/\lambda_p=0.016$ and $d=1.2\,\lambda_p$, with $\lambda_p=2\pi c/\omega_p$ a characteristic length. The frequency range corresponds to region D ($s$-polarized, backward SPPs). We see that in this range the real part of the SPP propagation constant is a decreasing function of the frequency and that it takes values which are almost identical to those corresponding to a flat surface, in agreement with the fact that, under these circumstances (low $h/d$ value, it reflects an specular order only) this grating is hardly distinguishable from a flat surface. We observe that the imaginary part of the propagation constant takes non-zero values even in the ideal case of lossless media ($\gamma=0$), which shows that the weak corrugation induces radiation losses corresponding to the onset of radiative spatial harmonics with $m=-1$ in both media and in the whole frequency range (see Eqs. (1) and (2)). As the frequency increases, the value of $|\mathrm{Im}\ \alpha(h, \omega)|$ decreases, indicating that for this material the radiation losses decrease with the frequency. Contrary to conventional, metallic SPPs, in this frequency range $\mathrm{Im}\ \alpha(h, \omega)<0$, which is a consequence of the backward nature of regime D. In this regime, the energy carried by the SPP must attenuate in the direction of the power flow ($-x$), that is, opposite to the propagation direction ($+x$, for our choice $\mathrm{Re}\ \alpha>0$), a situation identical to that of backward SPPs at a flat surface when the metamaterial has intrinsic losses [21]. In the realistic case $\gamma\neq 0$ we obtain greater values of $|\mathrm{Im}\alpha|$, in agreement with the fact that the SPP is now losing energy not only by radiation, but also because of the ohmic losses of the NRI metamaterial. Fig. 2c shows the specular reflectivity at normal incidence as a function of the incident frequency. The values obtained are almost identical to those corresponding to a surface without corrugation, except for frequencies near the spectral region –

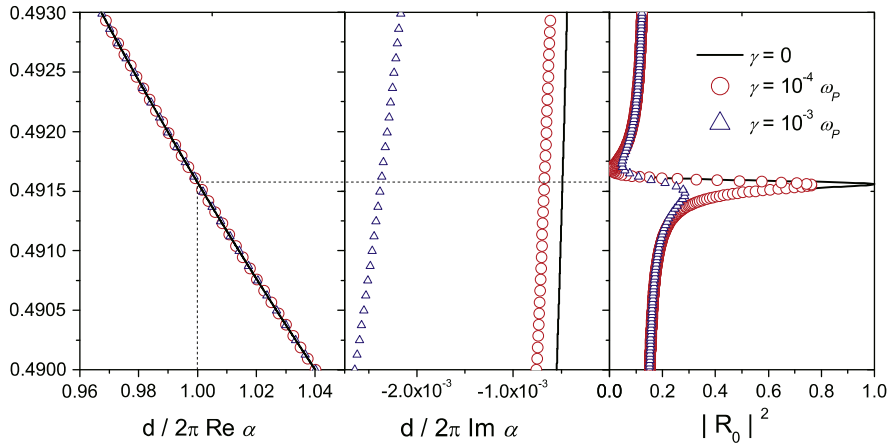


**Fig. 2.** (Color online) a) and b) Real and imaginary parts of the dimensionless propagation constant for backward SPPs propagating along a sinusoidal grating with $d=1.2\,\lambda_p$, $h_0=0.016\,\lambda_p$ ($\lambda_p=2\pi c/\omega_p$) and different values of the damping constant $\gamma$. c) Specular reflectivity at normal incidence as a function of the dimensionless angular frequency.

indicated by dotted lines in Fig. 2 – where the coupling condition (9) with $m=\pm 1$ holds. We observe that as the frequency increases, the coupling is dramatically manifested in abrupt reflectivity variations, changing from low values to a near unity maximum and then to an almost zero minimum. For the ideal case $\gamma=0$ the peak reflectance in the region of SPP resonance takes the maximum possible value (1, total reflection), but this value decreases when higher values of the damping constant $\gamma$ are considered. This kind of resonant behavior is very different from that exhibited by metallic gratings, for which reflectivity changes are quite symmetric near SPP resonances. The great asymmetry manifested by the presence of the maximum and the minimum observed in Fig. 2c seems to be characteristic of SPP regimes corresponding to almost transparent NRI corrugated gratings and has also been observed in reflectivity curves obtained at a fixed frequency for different angles of incidence [10].

In our second example we choose frequencies in the range $0.52<\omega/\omega_p<0.6$, corresponding to regime C ($p$-polarized, forward SPPs). Fig. 3 shows the SPP dispersion relation and the reflectivity curves obtained for gratingparameters identical to those considered in Fig. 2. The real part of the SPP propagation constant is an increasing function of the frequency, the same behavior observed in the forward regime for a flat boundary, and SPP losses are manifested in non-zero values for the imaginary part of the SPP propagation constant. This energy loss occurs not only because the NRI medium has ohmic losses but also because the SPP radiates towards adjacent media, as can be seen in Fig. 3b for the limit case $\gamma=0$. Contrary to the previous example, in this regime Im $\alpha>0$, in agreement with the forward nature of the SPP. Let us note that in this frequency range the radiation losses increase with the frequency, except near a discontinuity on the derivate of Im $\alpha$ at $\omega/\omega_p=0.5932$, where the spatial harmonic with $m=-1$ on the metamaterial side ceases to propagate. Fig. 3c shows the specular reflectivity in normal incidence. Since in this frequency range $0<\frac{d}{2\pi}\mathrm{Re}\ \alpha(h,\omega)b1$, Eq. (9) is no longer verified. Therefore, a coupling between the normally incident radiation and the SPP is not possible for these parameters and the reflectivity curve resembles that of the flat surface. The coupling condition can again be satisfied if the period of the corrugation is changed from value $d=1.2\,\lambda_p$ to $d=1.5\,\lambda_p$. Due to this coupling, Fig. 4 now presents a singular behavior for frequencies near the value predicted by Eq. (9) with $m=\pm 1$. The dotted horizontal and vertical lines in Fig. 4 help visualize the fulfillment of the coupling condition Eq. (9). We note that an almost total absorption is obtained for $\gamma=10^{-3}\omega_p$. When $\gamma$ increases from this value, we have observed (not shown in Fig. 4c) that the resonant effects in the reflectivity curve become less and less pronounced.

### 3.2. Asymmetric corrugations

We now consider asymmetric corrugations represented by $f(x)=\frac{h_0}{2}\sin(\frac{2\pi}{d}x)+\frac{h_1}{2}\sin(\frac{4\pi}{d}x)$, that is, a corrugation obtained by adding a first harmonic with amplitude $h_1$ to the sinusoidal surface

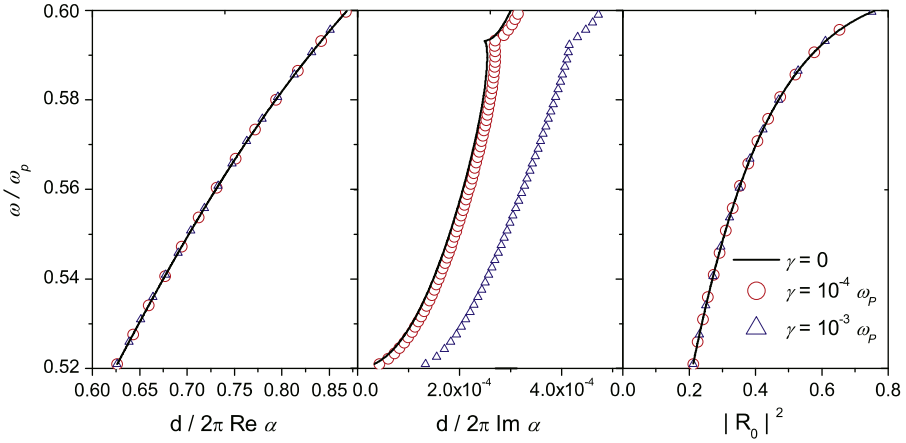


**Fig. 3.** (Color online) a) and b) Real and imaginary parts of the dimensionless propagation constant for forward SPPs propagating along a sinusoidal grating with $d=1.2\,\lambda_p$, $h_0=0.016\,\lambda_p$ and different values of the damping constant $\gamma$. c) Specular reflectivity at normal incidence as a function of the dimensionless angular frequency.

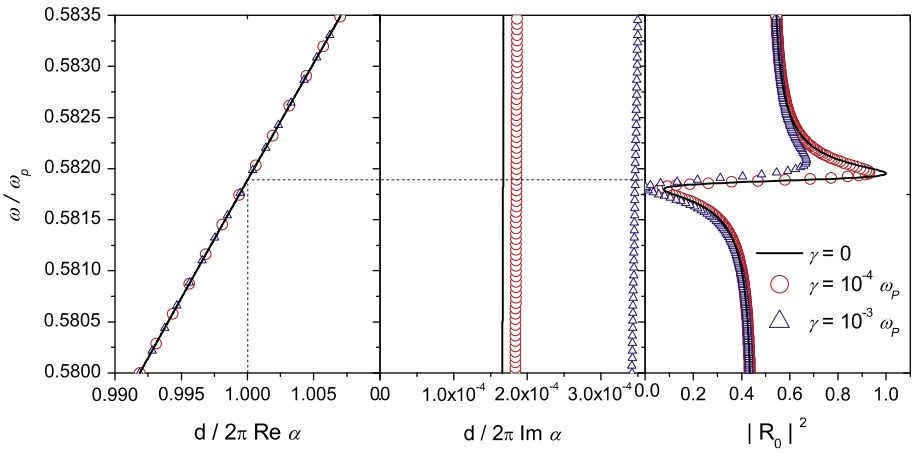


**Fig. 4.** (Color online) a) and b) Real and imaginary parts of the dimensionless propagation constant for forward SPPs propagating along a sinusoidal grating with $d = 1.5\,\lambda_p$, $h_0 = 0.016\,\lambda_p$ and different values of the damping constant γ. c) Specular reflectivity at normal incidence as a function of the dimensionless angular frequency.

previously considered in efsinusoidal. Fig. 5a and b shows the SPP dispersion curves obtained for $h_1 = h_0/3$, $d = 1.2\lambda_p$ and a frequency range corresponding to region D. As in the case of metallic gratings [12,18], the addition of the Fourier component with amplitude $h_1$ in the corrugation shape induces the formation of an SPP photonic band gap at frequencies near the value predicted by the Bragg condition Eq. (4) with $n = 2$. In this photonic band gap, indicated by the dotted horizontal lines in Fig. 5a and b, the absolute value of the imaginary part of the SPP is enhanced up to 10, 30 and 50 times the value taken outside the gap for $\gamma/\omega_p = 10^{-3}$, $10^{-4}$and0 respectively, and thus SPP propagation is practically inhibited. Note that, since Im $\alpha < 0$, the SPP keeps its backward nature. The presence of the gap in the dispersion curve is manifested in the reflectivity curve shown in Fig. 5c. Two singularities appear on the edges of the forbidden frequency interval, clearly evidencing the band gap limits. As γ increases these singularities become less and less pronounced. It should be noted that, similarly to the metallic case, the band gap limits are not evidenced when the SPP resonance is investigated in reflectivity experiments by scanning the angle of incidence at a constant frequency [18].

## 4. Conclusion

In conclusion, we have applied recently developed theoretical approaches to study i) the dispersive characteristics of SPPs supported by a corrugated boundary between a vacuum and a NRI material and ii) the electromagnetic response of this boundary when it is normally illuminated by a plane wave near conditions of SPP resonances. To consider material dispersion we have assumed that the electrical permittivity and the magnetic permeability of the NRI medium follow Drude and Lorentz models respectively and to evidence geometric dispersion we have studied two kinds of corrugation shapes, symmetric and asymmetric. We have verified that under certain coupling conditions (achieved by the choice of the corrugation period in our examples) the specular reflectivity of the NRI material dramatically changes, exhibiting the presence of a maximum and a minimum. Similar to the conventional case of metallic gratings, we have seen that the specific harmonic components of the grating profile can lead to very different SPP dispersion characteristics, leading in some cases to the formation of an SPP photonic band gap, that is, a frequency range in which SPP propagation is forbidden.

## Acknowledgments

This study is based on research supported by the Universidad de Buenos Aires (grant X062), Consejo Nacional de Investigaciones Científicas y Técnicas (CONICET) and Agencia Nacional de Promoción Científica y Tecnológica (BID 1728/OC–AR PICT-11–1785).

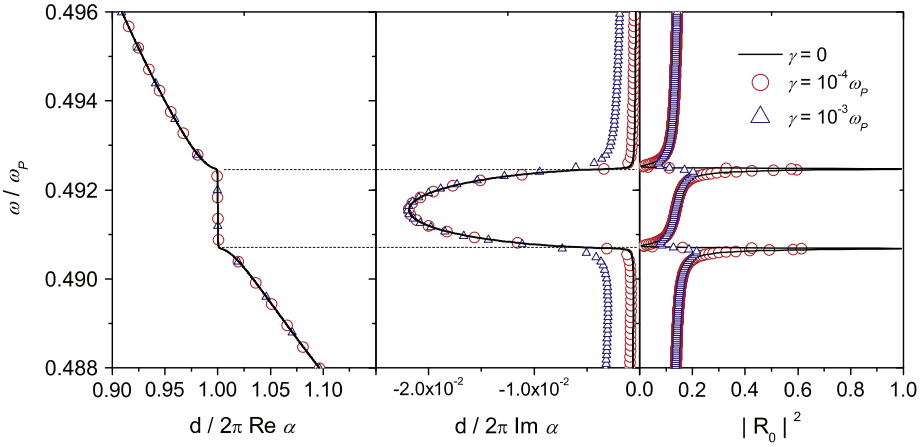


**Fig. 5.** (Color online) a) and b) Real and imaginary parts of the dimensionless propagation constant for forward SPPs propagating along a grating boundary given by $y = h_0/2\ sin(\frac{2\pi}{d}x) + h_1/2\ sin(\frac{4\pi}{d}x)$, with $d = 1.2\,\lambda_p$, $h_0 = 0.016\,\lambda_p$ and $h_1 = h_0/3$. c) Specular reflectivity at normal incidence as a function of the dimensionless angular frequency.

## References


[1] S.A. Maier, Plasmonics: Fundamentals and Applications, Springer, New York, 2007.
[2] L. Solymar, E. Shamonina, Waves In Metamaterials, Oxford University Press, New York, 2009.
[3] S.A. Darmanyan, M. Nevière, A.A. Zakhidov, Opt. Commun. 225 (2003) 233.
[4] R. Ruppin, Phys Letters A 277 (2000) 61.
[5] A. Ishimaru, S. Jaruwatanadilok, Y. Kuga, Prog. Eectromagn. Res. 51 (2005) 139.
[6] K. Park, B.J. Lee, C. Fu, Z.M. Zhang, J. Opt. Soc. Am. B 22 (2005) 1016.
[7] H. Zhang, Q. Wang, N. Shen, R. Li, J. Chen, J. Ding, H. Wang, J. Opt. Soc. Am. B 22 (2005) 2686.
[8] Fang-Fang Ren, Jing Chen, Du. Qing-Guo, Nian-hai Shen, Bi-Kan Tang, Hui-Tian Wang, Phys. Rev. B 75 (2007) 045127.
[9] P. Melezhik, A. Poyedinchuk, N. Yashina, G. Granet, J. Opt. A: Pure Appl. Opt. 9 (2007) S403.
[10] M. Cuevas, R.A. Depine, Phys. Rev. B 78 (2008) 125412.
[11] M. Cuevas, R.A. Depine, Phys. Rev. Lett. 103 (2009) 097401.
[12] W.L. Barnes, A. Dereux, T.W. Ebbesen, Nature 424 (2003) 824.
[13] A. Yelon, K.N. Piyakis, E. Sacher, Surf. Sci. 569 (2004) 47.
[14] M. Cuevas, R.A. Depine, Optik 122 (2011) 198.
[15] M. Cuevas, R.A. Depine, Eur. Phys. J. D 58 (2010) 249.
[16] R.A. Depine, A. Lakhtakia, Opt. Commun. 233 (2004) 277.
[17] R.A. Depine, A. Lakhtakia, Phys. Rev. E 69 (2004) 057602.
[18] W.L. Barnes, T.W. Preist, S.C. Kitson, J.R. Sambles, Phys. Rev. B 54 (1996) 6227.
[19] R.H. Ritchie, E.T. Arakawa, J.J. Cowan, R.N. Hamm, Phys. Rev. Lett. 21 (1968) 1530.
[20] N.E. Glass, M. weber, D.L. Mills, Phys. Rev. B 29 (1984) 6548.
[21] A. Ishimaru, J.R. Thomas, S. Jaruwatanadilok, IEEE Trans. Antennas Propag. 53 (2005) 915.